JCTC Journal of Chemical Theory and Computation

Using Hessian Updating To Increase the Efficiency of a Hessian Based Predictor-Corrector Reaction Path Following Method

H. P. Hratchian and H. B. Schlegel*

Department of Chemistry and Institute for Scientific Computing, Wayne State University, Detroit, Michigan 48202

Received June 15, 2004

Abstract: The reaction path is a key concept in the theoretical description of a chemical reaction. The intrinsic reaction coordinate is defined as the steepest descent path in mass-weighted Cartesian coordinates that connects the transition state to reactants and products on the potential energy surface. Recently, a new Hessian based predictor-corrector reaction path following algorithm was presented that is comparable to a fourth-order algorithm developed earlier. Although the method is very accurate, it is costly because second derivatives of the energy are required at each step. In this work, the efficiency of the method is greatly enhanced by employing Hessian updating. Three different updating schemes have been tested: Murtagh and Sargent, Powell-symmetric Broyden, and Bofill. Bofill's update performs the best and yields excellent speed-up.

1. Introduction

The theoretical treatment of chemical reactions invariably requires some sort of reaction path following calculation. The most common use of such a calculation is to ensure that an optimized transition state (TS) lies on a path connecting the desired reactant and product minima on the potential energy surface (PES). Additionally, accurate reaction path following methods are needed to determine the steepest descent path, or minimum energy path (MEP), so that variational transition state theory (VTST) and reaction path Hamiltonian (RPH) methods can be used to calculate reaction rate constants.[1−5] Although the steepest descent path can be considered in any coordinate system, when mass-weighted Cartesian coordinates are used the MEP is also known as the intrinsic reaction coordinate (IRC).[6]

The IRC can be determined by starting at the TS and following the steepest descent pathway down to the reactant and product minima according to

$$\frac{d\mathbf{x}(s)}{ds} = -\frac{\mathbf{g}(\mathbf{x})}{|\mathbf{g}(\mathbf{x})|} \qquad (1)$$

where s is the arc length along the path, $\mathbf{x}$ is the coordinate vector, and $\mathbf{g}$ is the gradient of the PES at $\mathbf{x}$. Because eq 1 is a stiff differential equation, care must be taken during the integration. As a result, a large number of algorithms have been developed.[7−22]

Numerical methods for integrating ordinary differential equations may be classified as either explicit or implicit. Explicit methods use information at the current point to move to the next point, while implicit methods required derivative information at the end point as well. For integrating eq 1, the differential equation defining the reaction path, common explicit algorithms include Euler's method, the Ishida-Morokuma-Komornicki (stabilized Euler) method,[11,12] Runge−Kutta, the local quadratic approximation (LQA),[15,16] and the Sun-Ruedenberg modification of LQA.[18] Some of these methods use only gradient information and are limited to rather small step sizes; others also use second derivatives (the Hessian). Methods that use the Hessian are more costly, but gain additional stability that permits somewhat larger step sizes.

Implicit methods are more difficult to implement because the gradient and possibly higher-order derivatives are necessary at the end of the step. As a result, implicit methods generally use optimization schemes to iteratively solve for

* Corresponding author e-mail: hbs@chem.wayne.edu.

10.1021/ct0499783 CCC: $30.25
Published on Web 10/21/2004

the derivatives at the end point of each step[23] and thereby tend to require multiple energy and derivative calculations for each point on the path. However, implicit methods are often able to take considerably larger steps allowing them to compensate for the cost of the additional derivative calculations. Implicit methods for IRC analysis include the Müller-Brown method (implicit Euler),[17] the second-order method of Gonzalez and Schlegel (GS2),[19,20] and higher-order methods by the same authors.[21]

In recent work, we introduced a new integrator for reaction path following.[24] Our Hessian based predictor-corrector (HPC) method provides a very accurate pathway and was originally designed to provide a useful approach for describing the reaction path for use in kinetics calculations (e.g., using VTST or RPH methods). In that work, it was shown that HPC is capable of step sizes comparable to the robust and widely used GS2 method. An attractive feature of the HPC integrator is that it only requires one evaluation of the energy and derivatives per IRC step, while the GS2 method typically requires between two and five energy and derivative evaluations per step in order to iteratively solve for the endpoint gradient. However, the original HPC algorithm requires Hessians at every step making it generally more expensive than GS2, which only requires first derivatives. In the present paper we remove this bottleneck by applying Hessian updating, and we show that this affords a very efficient and accurate means for computing IRCs. The approach here is to compute the Hessian analytically only at the TS and to update the second derivatives for the rest of the IRC integration. As we show below, using an appropriate updating scheme allows HPC step sizes similar to the popular GS2 integrator while only slightly diminishing the accuracy of the original HPC method (using all analytic Hessians). This indicates that the general HPC cost will be two to five times less than for GS2, since both methods can be used with similar step sizes and HPC with Hessian updating requires only one energy and gradient evaluation at each step. In this way, the HPC algorithm is not only useful for accurate reaction path following needed for rate constant calculations but is also efficient for those studies that require reaction path following primarily to ensure that an optimized TS lies on the pathway that connects the relevant reactant and product structures on the PES.

2. Method

In this work, we incorporate standard Hessian updating schemes into our Hessian based predictor-corrector (HPC) reaction path following algorithm, which has been previously described in detail.[24] In this section, the HPC method is briefly described, and the Hessian updating approaches are discussed.

A. Hessian Based Predictor-Corrector (HPC) Method. The HPC algorithm uses the local quadratic approximation (LQA) method of Page and McIver[15,16] for predictor steps and a modified Bulirsch-Stoer integrator[25−27] on a distance weighted interpolant (DWI) surface[28−30] for corrector steps. In this section, both pieces of the HPC method are discussed.

The LQA integrator is based upon a second-order Taylor series of the PES. Truncated at the quadratic term, the Taylor series expansion of the PES about $\mathbf{x_0}$ is given by

$$E(\mathbf{x}) = E_0 + \mathbf{g_0}^{\mathbf{t}}\Delta\mathrm{x} + \frac{1}{2}\Delta\mathrm{x}^{\mathbf{t}}\mathbf{H_0}\Delta\mathrm{x} \tag{2}$$

where $\Delta\mathbf{x}$, $\mathbf{g_0}$, and $\mathbf{H_0}$ are the displacement vector of the current position from $\mathbf{x_0}$, the gradient, and Hessian at $\mathbf{x_0}$, respectively. Taking the first derivative of eq 2 with respect to $\mathbf{x}$ gives the gradient as

$$\mathbf{g(x)} = \mathbf{g_0} + \mathbf{H_0}\Delta\mathrm{x} \tag{3}$$

Substituting eq 3 into eq 1 gives

$$\frac{\mathrm{d}\mathbf{x}(s)}{\mathrm{d}} = -\frac{\mathbf{g_0} + \mathbf{H_0}\Delta\mathrm{x}}{|\mathbf{g_0} + \mathbf{H_0}\Delta\mathrm{x}|} \tag{4}$$

In the LQA method of Page and McIver, eq 4 is integrated by introducing an independent parameter, t, such that

$$\frac{\mathrm{d}s}{\mathrm{d}t} = |\mathbf{g_0} + \mathbf{H_0}\Delta\mathrm{x}| \tag{5}$$

and

$$\frac{\mathrm{d}\mathbf{x}}{\mathrm{d}t} = -[\mathbf{g_0} + \mathbf{H_0}\Delta\mathrm{x}] \tag{6}$$

The solution to eq 6 is given by

$$\mathbf{x}(t) = \mathbf{x_0} + \mathbf{A}(t)\mathbf{g_0} \tag{7}$$

where

$$\mathbf{A}(t) = \mathbf{U}\alpha(t)\mathbf{U}^{\mathbf{t}} \tag{8}$$

In eq 8, $\mathbf{U}$ is the matrix of column eigenvectors of the Hessian and $\alpha(t)$ is a diagonal matrix given by

$$\alpha_{ii}(t) = (e^{-\lambda_i t} - 1)/\lambda_i \tag{9}$$

where λ_i are the eigenvalues of the Hessian.

To integrate eq 4, one must obtain a value of t such that the desired step size $(s - s_0)$ is taken. To accomplish this, iterations over successive Euler integrations of eq 5 are used. The initial value for the Euler step size, δt, is estimated by

$$\delta t = \frac{1}{N_{Euler}}\frac{(s - s_0)}{|\mathbf{g_0}|} \tag{10}$$

where N_{Euler} is the number of Euler steps to be taken. In the present implementation, $N_{Euler} = 5000$. The numerical integration of eq 5 can be carried out readily in the Hessian eigenvector space

$$\frac{\mathrm{d}s}{\mathrm{d}t} = \left(\sum_i \mathbf{g'_{0_i}}^2 e^{-2\lambda_i t}\right)^{1/2} \tag{11}$$

where

$$\mathbf{g'_0} = \mathbf{U}^{\mathbf{t}}\mathbf{g_0} \tag{12}$$

At the start of the integration, when **x** corresponds to the TS, the gradient is zero, and hence the transition vector must be used in place of $\mathbf{g_0}$. At the TS, the LQA step is equivalent to the gradient extremal step, as described by Hoffman, Nord, and Ruedenburg.[31] At the end of the LQA integration, when **x** approaches the minimum wells of the reactant and product, t heads to infinity and the LQA step is equivalent to a Newton−Raphson step, which leads to the minimum energy structure in the local quadratic region. For this reason, conservation of the desired step size, $(s - s_0)$, becomes difficult in this region. Therefore, once the calculation has moved beyond the quadratic region of the TS each LQA step is compared to a Newton−Raphson step. When the Newton−Raphson step is shorter than the LQA step, the Newton−Raphson step is taken in lieu of the LQA step. This provides convergence stability for the corrector step (see below) when the minimum well is approached.

The Bulirsch-Stoer integrator, which is very well described elsewhere,[25−27,32] is used for the HPC corrector step. Each Bulirsch-Stoer step is comprised of three basic components. First, a simple gradient based integrator is used to take multiple steps along the Bulirsch-Stoer step interval. In general, this integrator is modified midpoint; however, in our tests we found that the stiff character of eq 1 is greatly magnified by modified midpoint. Therefore, our modified version employs simple Euler integration. A detailed discussion of the causes for Euler integration being more stable than modified midpoint is available in previous work.[24] The second component of a Bulirsch-Stoer step is to describe the solution of the Euler integration as a polynomial function of step size and to extrapolate to a step size of zero (corresponding to the case where an infinite number of steps are taken). The third component consists of evaluating the error of the extrapolation to zero step size. If the error is too large, the process is repeated using more steps in the Euler integration, which in turn provides one more data set for the polynomial extrapolation. If the error is acceptable ($<1 \times 10^{-6}$ amu$^{1/2}$ bohr in the present case), then the extrapolated solution is accepted and the integration is completed.

This integrator requires a large number of function and gradient evaluations and can be quite costly if energies and derivatives are required from electronic structure methods. However, in the present algorithm the Bulirsch-Stoer integration is carried out on a surface that is fitted to energy and derivative information already available at the beginning and end of the predictor step (LQA). Once the Bulirsch-Stoer integration is completed and the LQA end point is corrected, the gradient on the fitted surface is used to take the next LQA predictor step. Since the corrected end point and predicted end point are expected to lie within the same quadratic region of the PES, the Hessian from the previous predictor end point is used for the next LQA step. The validity of this assumption has been demonstrated in previous work.[24,33,34]

In the current algorithm, the Bulirsch-Stoer integration is carried out on a DWI surface such as those described by Collins and co-workers.[30,35−37] DWI surfaces have been used in a number of diverse applications[38] and are well suited for modeling chemical PESs.[30] This fitted surface gives the interpolated energy, E_{DWI}, at a position **x** according to

$$E_{DWI} = \sum_{i=1}^{2} w_i T_i \tag{13}$$

where the summation is taken over the start (i=1) and end (i=2) points of the predictor step, about which Taylor expansions, $\{T_i\}$, are evaluated and added together in a weighted fashion, defined by the weighting functions $\{w_i\}$. In the present implementation, the two Taylor expansions are truncated at the second-order term and the weighting functions are defined as

$$w_1 = \frac{|\Delta x_2|^2}{|\Delta x_1|^2 + |\Delta x_2|^2},\ w_2 = \frac{|\Delta x_1|^2}{|\Delta x_1|^2 + |\Delta x_2|^2} \tag{14}$$

B. Hessian Updating Methods. To study larger and more interesting systems with electronic structures methods, the efficiency of the HPC algorithm must be improved. To accomplish the same goal, Hessian updating methods have been utilized in the past with great success with quasi-Newton geometry optimization methods[8,39−41] and ab initio classical trajectory calculations.[34] Furthermore, other reaction path following methods have been able to make good use of Hessian updating.[9,19−21,42] These prior successes indicate that, for HPC, Hessian updating may provide a means to decrease computational cost, especially for applications where Hessians are not needed for additional calculations at each point on the path and users intend to obtain the IRC only to ensure that an optimized TS lies on a pathway connecting reactants to products. Nevertheless, careful consideration must be given to the choice of updating scheme since the updated Hessians will not only be used to propagate the IRC via LQA, but HPC also requires Hessians to fit the DWI surface for the modified Bulirsch-Stoer corrector integration. A poorly updated Hessian may lead to an inaccurate DWI surface, severely disturb the corrector integration, and provide an inadequate gradient for the next LQA predictor step.

For minimizations, the BFGS Hessian updating scheme is preferred.[43,44] A principle reason for this preference is that the BFGS formula maintains a Hessian that is positive definite. This characteristic of the BFGS formula is achieved by employing positive weights that are functions of the current Hessian. In the case of reaction path following, the Hessian will be negative definite in some regions (i.e., near the TS) and the BFGS formula becomes ill-conditioned.[45] As a result, Hessian updating methods that have been used for TS optimization problems are more appropriate and have been considered. In this work, three different Hessian updating schemes have been incorporated with HPC to determine which, if any, provides an acceptable integration of the IRC while affording the desired increase in efficiency.

The first updating scheme used is the method of Murtagh and Sargent (MS), which is also known as the symmetric rank one formula (SR1). The MS update is given by

$$\Delta\mathbf{H}_{MS} = \mathbf{H}^{new} - \mathbf{H}^{old} = \frac{(\Delta g - \mathbf{H}^{old}\Delta x)(\Delta g - \mathbf{H}^{old}\Delta x)^t}{(\Delta g - \mathbf{H}^{old}\Delta x)^t \Delta x} \quad (15)$$

For optimization on a quadratic surface, MS updating converges to the correct Hessian without exact line searches.[43,44] However, care must be taken to avoid MS updating if the denominator of eq 15 becomes small.

Alternatively, the Powell-symmetric-Broyden (PSB) updating method can be employed. The PSB update is

$$\Delta\mathbf{H}_{PSB} = \frac{(\Delta g - \mathbf{H}^{old}\Delta x)\Delta x^t + \Delta x(\Delta g - \mathbf{H}^{old}\Delta x)^t}{\Delta x^t \Delta x} - \frac{\Delta x^t(\Delta g - \mathbf{H}^{old}\Delta x)\Delta x \Delta x^t}{(\Delta x^t \Delta x)^2} \quad (16)$$

The PSB updating scheme is free from the possibility of division by zero, unlike the MS update. Another Hessian updating approach that also avoids the division by zero problem of MS updating is Bofill's formula, which combines the MS and PSB schemes.[46] Bofill's update was devised as an alternative updating scheme for TS optimizations and is given by

$$\Delta\mathbf{H}_{Bofill} = \phi\Delta H_{MS} + (1 - \phi)\Delta\mathbf{H}_{PSB} \quad (17)$$

where

$$\phi = \frac{(\Delta x^t(\Delta g - \mathbf{H}^{old}\Delta x))^2}{\Delta x^2(\Delta g - \mathbf{H}^{old}\Delta x)^2} \quad (18)$$

An alternative form for Bofill's update has been proposed by Farkas and Schlegel.[47,48] In their approach, ϕ is given by the square root of eq 18. For HPC reaction path following, the modified Bofill update provides similar results to the standard Bofill method. As a result, this update is not explicitly considered in this work.

3. Numerical Tests

The HPC algorithm and the three Hessian updating schemes discussed above have been implemented in the development version of GAUSSIAN 03.[49] Aside from the Hessian at the TS, which is computed analytically, all Hessians are obtained by updating during the HPC reaction path calculation. Four systems have been employed for testing: HCN → HNC, $CH_3CH_2F \rightarrow CH_2CH_2 + HF$, $ClCH_3 + Cl^- \rightarrow Cl^- + CH_3Cl$, and the Diels−Alder reaction of ethene and butadiene. Calculations on the HCN rearrangement reaction have been carried out at the HF/STO-3G level of theory,[50,51] those on the four center elimination reaction have been carried out at the HF/3-21G level of theory,[52−54] and calculations on $ClCH_3 + Cl^- \rightarrow Cl^- + CH_3Cl$ and the Diels−Alder reaction have been carried out at the HF/6-31G(d) level of theory.[55−59] Because the masses of the atoms that dominate the reaction path are quite different for these four reactions, a fixed step size in mass-weighted coordinates would correspond to significantly different step sizes in nonmass-weighted coordinates. However, the trust radii for the quadratic regions of the four reactions should be similar when expressed in nonmass-weighted coordinates. Therefore, we chose a step size in nonmass-weighted coordinates at the TS, transformed it to mass-weighted coordinates, and used it for the rest of the path. In particular, we selected step sizes of 0.10 and 0.40 bohr for each of the four test reactions.

As an initial test for the accuracy of IRCs computed using HPC integration with the three updating schemes described above, we compared plots of energy vs reaction coordinate and various internal coordinates vs reaction coordinate with the HPC paths computed using all analytic Hessians. In these tests, the paths were computed from the respective TSs down to reactant and product minima, which were detected according to one of two stopping criteria: (1) the magnitude of the Cartesian gradient is less than 1.5×10^{-4} Hartree bohr^{-1} or (2) the angle between two successive steps is less than 30°.

Visual inspection indicates that in the region near the TS all three updating methods yield very good pathways when compared to the path using all analytic Hessians. Near the endpoints (i.e., the reactant and product wells), the PSB and Bofill schemes perform well, while the MS updates result in large deviations from the reference pathway for some reactions. Here, we show plots for two reactions that are representative of the set studied. Figures 1 and 2 relate to the HCN rearrangement reaction. Figures 1(a) and 2(a) give the (x,y) coordinates of the H atom, where the C−N center of mass has been placed at the origin, the C−N bond has been placed on the x-axis, the C atom has been placed on the negative side of the x-axis, and the N atom has been placed on the positive x-axis. Figures 1(b) and 2(b) show the C−N bond length as a function of the reaction coordinate. Figures 3(a) and 4(a) show energy profiles for the four center elimination reaction, $CH_3CH_2F \rightarrow CH_2CH_2 + HF$. Figures 1(c), 2(c), 3(b), and 4(b) show the errors in the pathways, given by the perpendicular distance from the paths computed with all analytic Hessians, as a function of reaction coordinate.

It is clear from Figures 1 and 3 that with a step size of 0.10 bohr PSB and Bofill updating schemes both yield very good paths. MS updating does well with the four center elimination reaction with the smaller step size but yields long C−N bonds for the HCN rearrangement. For the paths integrated with a step size of 0.40 bohr, the behavior of the three updating schemes is qualitatively similar to the results from integration with a step size of 0.10 bohr. As one might expect, slight deviations from the reference path for PSB and Bofill updating with the smaller step size become somewhat more apparent when the larger step size is used. Nevertheless, agreement of the paths found using these two updating schemes with the analytic Hessian pathway is still acceptable. The errors in the MS updating paths remain small for the four center elimination reaction but are much larger for the HCN rearrangement. As shown in Figures 1(c) and 2(c), the errors in the MS pathways for the HCN rearrange-

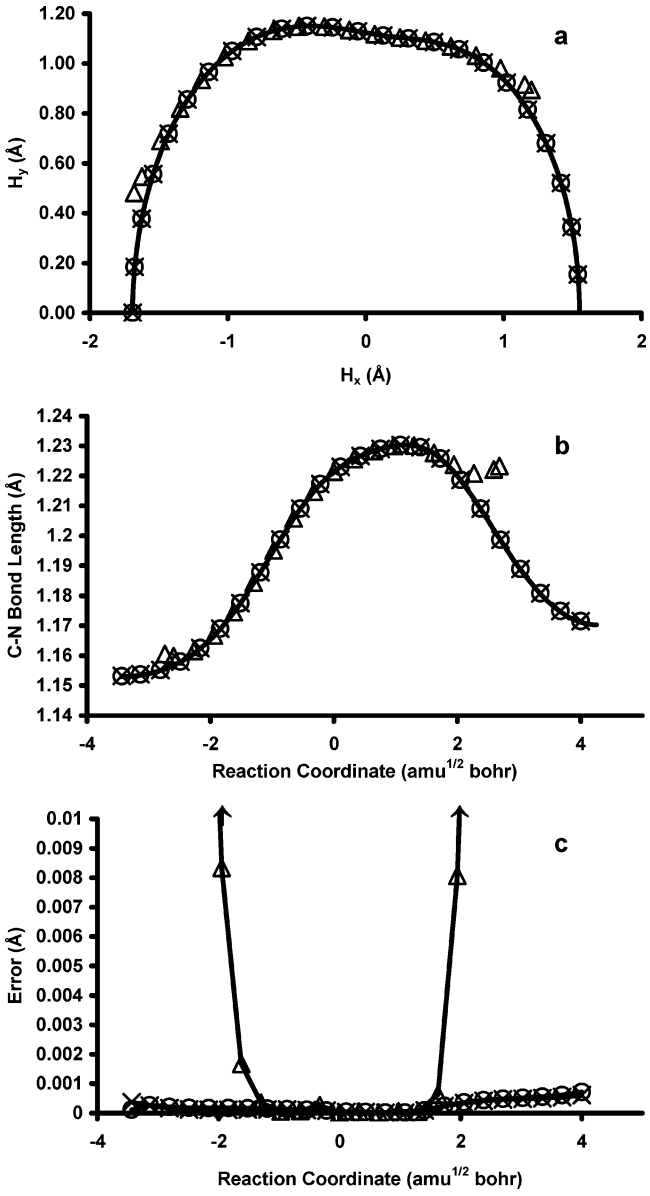

Figure 1. Reaction path for HCN → HNC with all analytic Hessians vs all updated Hessians using a step size of 0.10 bohr. (a) Coordinates of H atom relative to the C−N center of mass, (b) C−N bond length vs reaction coordinate, and (c) error, given by perpendicular distance from the all analytic Hessian path, vs reaction coordinate [HPC paths using analytic Hessians (—), MS updated Hessians (△), PSB updated Hessians (○), Bofill updated Hessians (×)]. Note: plot (c) shows solid lines connecting points for MS, PSB, and Bofill updated paths for clarity. Every third point is shown for simplicity (for all three plots).

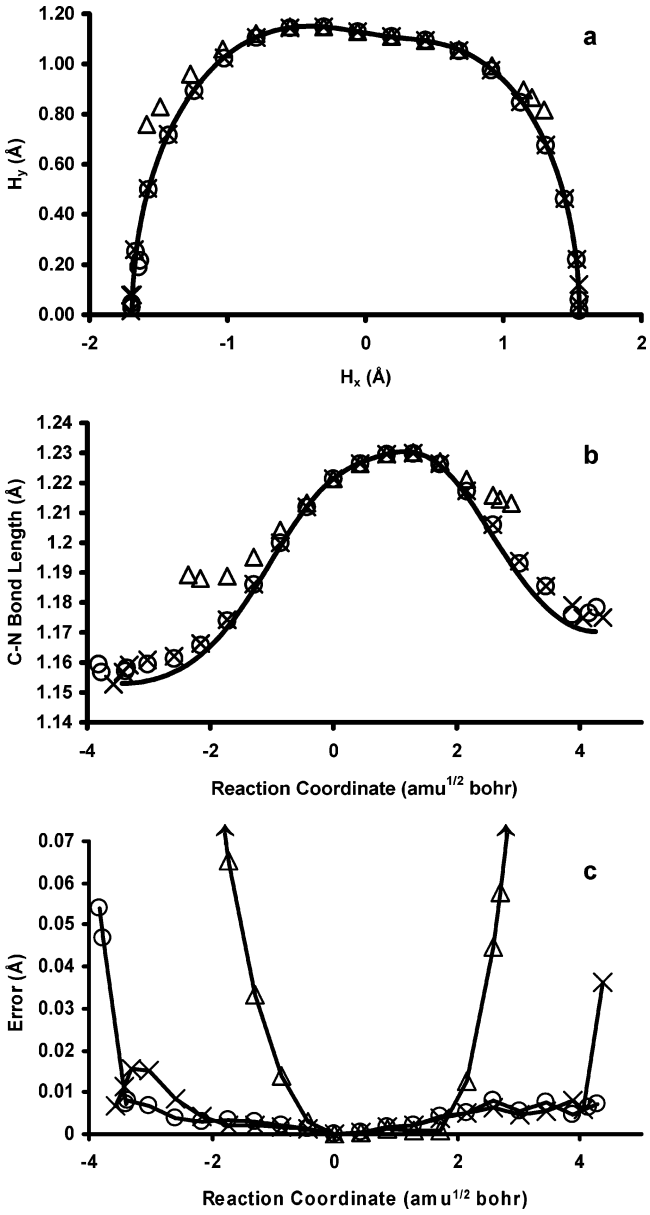

Figure 2. Reaction path for HCN → HNC with all analytic Hessians vs all updated Hessians using a step size of 0.40 bohr. (a) Coordinates of H atom relative to the C−N center of mass, (b) C−N bond length vs reaction coordinate, and (c) error, given by perpendicular distance from the all analytic Hessian path, vs reaction coordinate [HPC paths using analytic Hessians (—), MS updated Hessians (△), PSB updated Hessians (○), Bofill updated Hessians (×)]. Note: plot (c) shows solid lines connecting points for MS, PSB, and Bofill updated paths for clarity.

ment rapidly extend beyond the vertical scale of the plot as the reactant and product valleys are approached.

For both reactions, the MS paths prematurely detect minima wells and terminate. In the case of the HCN rearrangement, the calculation detects the reactant well before the H−C−N angle has reached 180°. Calculations on the four center elimination reaction end early heading toward the product when the larger step size is used and end early in the reactant direction with both step sizes. We have found that this is a common problem with MS updating, which is clearly apparent in Figures 1−4. In all cases, the calculations terminated according to the first stopping criteria listed above—the magnitude of the Cartesian gradient is less than 1.5×10^{-4} Hartree bohr^{-1}. As mentioned earlier, the gradient used in each HPC predictor step comes from the DWI gradient at the end point from the previous corrector step. Consequently, a poor Hessian can result in a local minimum on the DWI surface and artificially cause the calculation to complete.

The problems experienced using MS updating can be corrected by computing analytic Hessians every few steps.

Table 1. RMS Errors in Position (Å) for HPC Reaction Path Following Using MS, PSB, and Bofill Hessian Updating Methods with $\Delta s = 0.10$ and 0.40 bohr[a]

		Hessian updating method		
reaction	step size	MS	PSB	Bofill
HNC → HCN	0.10	3.36×10^{-2}	3.35×10^{-4}	3.05×10^{-4}
	0.40	6.96×10^{-2}	1.60×10^{-2}	1.05×10^{-2}
$CH_3CH_2F \rightarrow CH_2CH_2 + HF$	0.10	8.55×10^{-3}	2.58×10^{-3}	4.73×10^{-3}
	0.40	5.78×10^{-2}	6.56×10^{-2}	8.46×10^{-2}
$ClCH_3 + Cl^- \rightarrow Cl^- + CH_3Cl$	0.10	2.33×10^{-2}	1.09×10^{-2}	3.04×10^{-3}
	0.40	*b*	1.21×10^{-1}	3.46×10^{-2}
Diels–Alder	0.10	1.94×10^{-2}	1.38×10^{-2}	1.58×10^{-2}
	0.40	6.35×10^{-2}	8.33×10^{-2}	9.50×10^{-2}

[a] $\Delta s = 0.10$ and 0.40 bohr correspond to 0.1082 and 0.4326 $amu^{1/2}$ bohr for HNC → HCN; 0.1090 and 0.4362 $amu^{1/2}$ bohr for $CH_3CH_2F \rightarrow CH_2CH_2 + HF$; 0.3545 and 1.4182 $amu^{1/2}$ bohr for $ClCH_3 + Cl^- \rightarrow Cl^- + CH_3Cl$; and 0.2524 and 1.0098 $amu^{1/2}$ bohr for the Diels–Alder reaction. [b] The integration of eq 1 failed for this calculation.

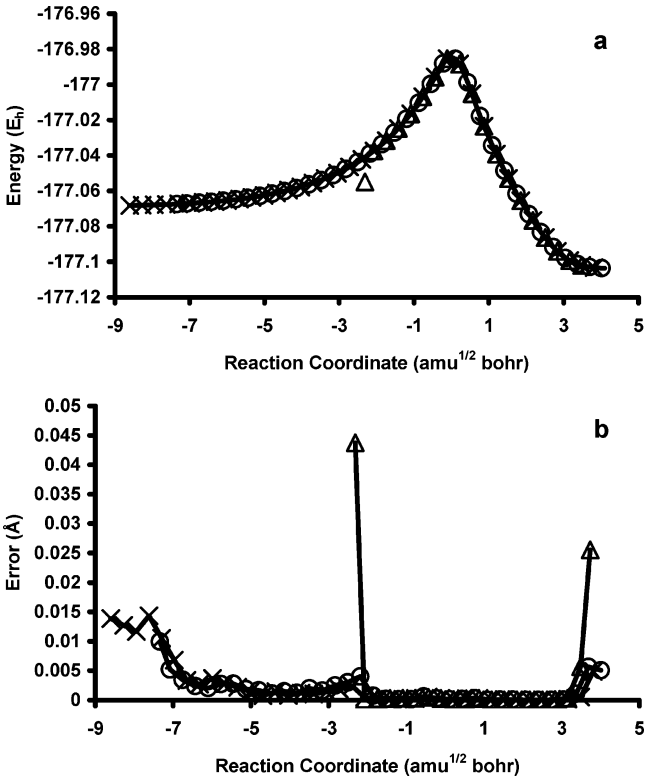

Figure 3. Reaction path for $CH_3CH_2F \rightarrow CH_2CH_2 + HF$ with all analytic Hessians vs all updated Hessians using a step size of 0.10 bohr. (a) Energy profile and (b) error, given by perpendicular distance from the all analytic Hessian path, vs reaction coordinate [HPC paths using analytic Hessians (—), MS updated Hessians (△), PSB updated Hessians (○), Bofill updated Hessians (×)]. Every third point is shown for simplicity.

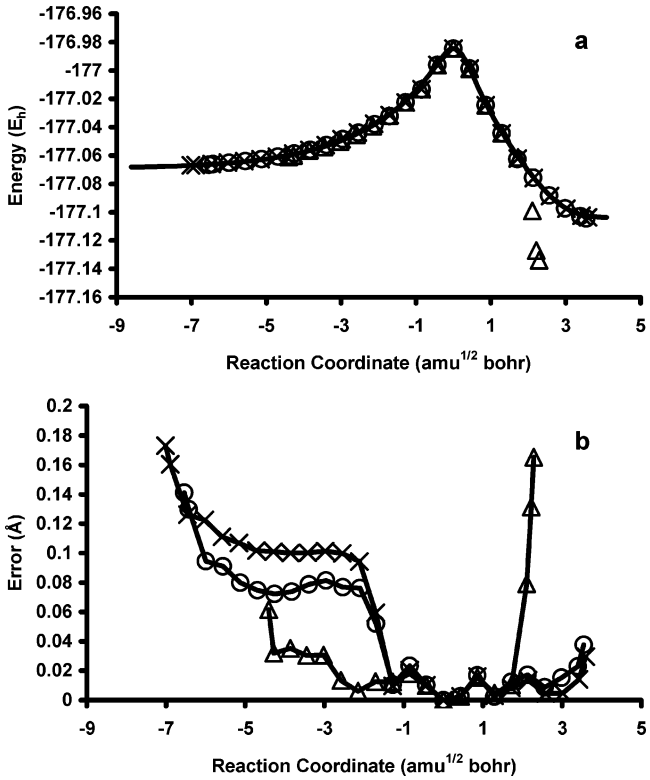

Figure 4. Reaction path for $CH_3CH_2F \rightarrow CH_2CH_2 + HF$ with all analytic Hessians vs all updated Hessians using a step size of 0.40 bohr. (a) Energy profile and (b) error, given by perpendicular distance from the all analytic Hessian path, vs reaction coordinate [HPC paths using analytic Hessians (—), MS updated Hessians (△), PSB updated Hessians (○), Bofill updated Hessians (×)].

Specifically, we have found that updating at least once every five steps provides very good agreement with the all analytic Hessian pathways. One could also recompute the Hessian whenever the rms change in matrix elements is larger than a threshold.[42] Both options have been included in this implementation of the method. Nevertheless, PSB and Bofill updating methods work well enough for the reactions considered in this paper that no analytic Hessians are required during the course of the IRC integration, except at the TS.

Although Figures 1–4 provide a qualitative measure of the accuracy, a quantitative measure of the accuracy of each updating scheme is desirable. To this end, we have computed the perpendicular distance between points on the updated Hessian and analytic Hessian pathways, which are reported in Table 1.

The inferiority of MS updating is clear from the data provided in Table 1. Indeed, for the HCN rearrangement reaction (using the smaller step size) the errors in the paths are roughly 2 orders of magnitude greater for MS than for Bofill and PSB [see Figure 1(c)]. For the four center elimination [see Figure 3(b)] and Diels–Alder reactions, all three updating schemes essentially perform the same, while the symmetric S_N2 reaction has RMS errors in position that

Table 2. Comparison of Relative CPU Time for HPC Calculations Using All Analytic Hessians vs Those Using All Updated Hessians[a]

reaction	no. of basis functions	relative time for all analytic Hessians	relative time for all updated Hessians
HNC → HCN	11	1.00	0.66
$CH_3CH_2F \rightarrow CH_2CH_2 + HF$	37	1.46	0.86
$ClCH_3 + Cl^- \rightarrow Cl^- + CH_3Cl$	59	5.51	1.77
Diels−Alder	110	61.12	7.41
CpCoMeNO → CpCoNMeO	388	5104.95	533.54

[a] All cases start with an analytic Hessian at the transition state.

considerably larger when MS and PSB updating are used as compared to Bofill updating for this step size. For the larger step size, the errors from paths using all three updating methods are much larger than the cases where the smaller step size is employed in the integration. These differences in errors are approximately 1 and 2 orders of magnitude. Additionally, the superiority of PSB and Bofill updating schemes over MS is not, in general, as clear when a larger integration step is used. In fact, for the four center elimination reaction the MS path is better than the PSB or Bofill paths, although the differences in errors for each path are small.

It is worth noting that the path errors due to Hessian updating (Table 1) are only slightly larger than the path errors previously measured for paths using all analytic Hessians at similar step sizes.[24] This indicates that using all updated Hessians only slightly decreases the accuracy of the IRC and that HPC with Hessian updating is capable of integrating the IRC using a step size that is similar to GS2. With Hessian updating, HPC requires only one energy and one gradient evaluation per step, making HPC very competitive with GS2 and other popular IRC integrators.

Since the data suggest that updating using Bofill's formula is, for most applications, superior to the other methods considered, the Bofill updating scheme has been chosen as the default scheme for HPC with Hessian updating. As previously stated, the impetus for this work is to increase the efficiency of HPC to allow its use in studies of large and interesting systems. Therefore, the relative speed-up due to updating (using the Bofill updating scheme) has been investigated. Table 2 shows relative CPU times for calculating 40 steps in the forward direction and 40 steps in the reverse direction for the HCN rearrangement, four center elimination, symmetric S_N2, and Diels−Alder reactions. The choice of the number of steps is completely arbitrary and is kept uniform among the reactions considered to provide for better cost comparison and determination of basis set size dependence. Table 2 also shows the relative cost for the insertion of NO into a Co−CH_3 σ bond, which has been previously studied by Hall and co-workers.[60−62] In this work, we have employed the B3LYP/6-311G(d,p) level of theory.[63−66] Due to the size of this system we have only calculated paths with 25 steps in the forward direction and 25 steps in the reverse direction.

As expected, updating the Hessian provides large decreases in computational cost. The degree of speed-up afforded by Hessian updating is dependent on the size of the system studied. This is expected since the bottleneck in the all analytic Hessian calculations is Hessian evaluation and the bottleneck in the updated Hessian calculations is the computation of the energy and gradient. Therefore, the speed-up due to Hessian updating will depend on the differential between the energy and Hessian calculations. For the HCN rearrangement reaction (11 basis functions) the decrease in cost for the calculation with all updated Hessians is roughly 34%, while using updated Hessians for the NO insertion reaction—the largest system studied here (388 basis functions)—provides nearly an order of magnitude speed-up.

4. Conclusions

In this paper, the efficiency of our Hessian predictor-corrector reaction path following algorithm has been improved by utilizing Hessian updating, making it an attractive alternative to other commonly used IRC integrators. In every case considered, the Hessian has been calculated analytically only at the TS. All subsequent steps have used updated Hessians. The relative performance of three popular Hessian updating schemes was investigated, and it was determined that the best method is the Bofill update. Using this updating approach, the relative CPU speed-up for HPC calculations on five different reactions was studied. For the smallest system considered, HCN rearrangement, a relative speed-up of roughly a factor of 1.3 was observed. For the largest system studied, NO insertion into a Co−CH_3 σ bond, nearly an order of magnitude speed-up was accomplished.

Acknowledgment. H.P.H. thanks the Institute for Scientific Computing at Wayne State University for support provided by a NSF-IGERT Fellowship. This work was supported by a grant from the NSF (CHE 0131157).

References

(1) Garrett, B. C.; Truhlar, D. G. In *Encyclopedia of Computational Chemistry*; Schleyer, P. v. R., Allinger, N. L., Kollman, P. A., Clark, T., Schaefer, H. F., III, Gasteiger, J., Schreiner, P. R., Eds.; Wiley: Chichester, 1998; pp 3094−3104.

(2) Truhlar, D. G.; Garrett, B. C. *Annu. Rev. Phys. Chem.* **1984**, *35*, 159−189.

(3) Truhlar, D. G.; Garrett, B. C.; Klippenstein, S. J. *J. Phys. Chem.* **1996**, *100* (31), 12771−12800.

(4) Miller, W. H.; Handy, N. C.; Adams, J. E. *J. Chem. Phys.* **1980**, *72* (1), 99−112.

(5) Kraka, E. In *Encyclopedia of Computational Chemistry*; Schleyer, P. v. R., Allinger, N. L., Kollman, P. A., Clark, T., Schaefer, H. F., III, Gasteiger, J., Schreiner, P. R., Eds.; Wiley: Chichester, 1998; pp 2437−2463.

(6) Fukui, K. *Acc. Chem. Res.* **1981**, *14* (12), 363−368.

(7) McKee, M. L.; Page, M. *Rev. Comp. Chem.* **1993**, 4, 35−65.

(8) Schlegel, H. B. In *Modern Electronic Structure Theory*; Yarkony, D. R., Ed.; World Scientific: Singapore, 1995.

(9) Schlegel, H. B. In *Encyclopedia of Computational Chemistry*; Schleyer, P. v. R., Allinger, N. L., Clark, T., Gasteiger, J., Kollman, P. A., Schaefer, H. F., III, Schreiner, P. R., Eds.; Wiley: Chichester, 1998; pp 2432−2437.

(10) Collins, M. A. *Adv. Chem. Phys.* **1996**, *93*, 389−453.

(11) Schmidt, M. W.; Gordon, M. S.; Dupuis, M. *J. Am. Chem. Soc.* **1985**, *107*, 2585−2589.

(12) Ishida, K.; Morokuma, K.; Komornicki, A. *J. Chem. Phys.* **1977**, *66*, 2153-2156.

(13) Baldridge, K. K.; Gordon, M. S.; Steckler, R.; Truhlar, D. G. *J. Phys. Chem.* **1989**, *93*, 5107−5119.

(14) Garrett, B. C.; Redmon, M. J.; Steckler, R.; Truhlar, D. G.; Baldridge, K. K.; Bartol, D.; Schidt, M. W.; Gordon, M. S. *J. Phys. Chem.* **1988**, *92*, 1476−1488.

(15) Page, M.; McIver, J. M. *J. Chem. Phys.* **1988**, *88* (2), 922−935.

(16) Page, M.; Doubleday: C.; McIver, J. W. *J. Chem. Phys.* **1990**, *93* (8), 5634−5642.

(17) Müller, K.; Brown, L. D. *Theor. Chim. Acta* **1979**, *53*, 75−93.

(18) Sun, J. Q.; Ruedenberg, K. *J. Chem. Phys.* **1993**, *99*, 5269−5275.

(19) Gonzalez, C.; Schlegel, H. B. *J. Chem. Phys.* **1989**, *90* (4), 2154−2161.

(20) Gonzalez, C.; Schlegel, H. B. *J. Phys. Chem.* **1990**, *94* (14), 5523−5527.

(21) Gonzalez, C.; Schlegel, H. B. *J. Chem. Phys.* **1991**, *95* (8), 5853−5860.

(22) Schlegel, H. B. *J. Comp. Chem.* **2003**, *24*, 1514−1527.

(23) Gear, C. W. *Numerical Initial Value Problems in Ordinary Differential Equations*; Prentice Hall: Englewood Cliffs, 1971.

(24) Hratchian, H. P.; Schlegel, H. B. *J. Chem. Phys.* **2004**, *120* (21), 9918−9924.

(25) Bulirsch, R.; Stoer, J. *Num. Math.* **1964**, *6*, 413−427.

(26) Bulirsch, R.; Stoer, J. *Num. Math.* **1966**, *8*, 1−13.

(27) Bulirsch, R.; Stoer, J. *Num. Math.* **1966B**, *8*, 93−104.

(28) Farwig, R. *Math Comput.* **1986**, *46*, 577.

(29) Farwig, R. In *Algorithms for approximation*; Mason, J., Cox, M., Eds.: Clarendon, Oxford, 1987; p 194.

(30) Collins, M. A. *Theor. Chem. Acc.* **2002**, *108* (6), 313−324.

(31) Hoffman, D. K.; Nord, R. S.; Ruedenberg, K. *Theor. Chim. Acta* **1986**, *69* (4), 265−279.

(32) Press, W. H. *Numerical recipes in FORTRAN 77: the art of scientific computing*; Cambridge University Press: Cambridge [England]; New York, 1996.

(33) Millam, J. M.; Bakken, V.; Chen, W.; Hase, W. L.; Schlegel, H. B. *J. Chem. Phys.* **1999**, *111* (9), 3800−3805.

(34) Bakken, V.; Millam, J. M.; Schlegel, H. B. *J. Chem. Phys.* **1999**, *111* (19), 8773−8777.

(35) Bettens, R. P. A.; Collins, M. A. *J. Chem. Phys.* **1999**, *111* (3), 816−826.

(36) Thompson, K. C.; Jordan, M. J. T.; Collins, M. A. *J. Chem. Phys.* **1998**, *108* (2), 564−578.

(37) Ischtwan, J.; Collins, M. A. *J. Chem. Phys.* **1994**, *100* (11), 8080−8088.

(38) Lancaster, P.; Salkauskas, K. *Curve and Surface Fitting: An Introduction*; Academic Press: London; Orlando, 1986.

(39) Schlegel, H. B. *J. Comp. Chem.* **1982**, *3* (2), 214.

(40) Schlegel, H. B. In *Encyclopedia of Computational Chemistry*; Schleyer, P. v. R., Allinger, N. L., Kollman, P. A., Clark, T., Schaefer, H. F., III, Gasteiger, J., Schreiner, P. R., Eds.; Wiley: Chichester, 1998; pp 1136−1142.

(41) Schlick, T. In *Encyclopedia of Computational Chemistry*; Schleyer, P. v. R., Allinger, N. L., Kollman, P. A., Clark, T., Schaefer, H. F., III, Gasteiger, J., Schreiner, P. R., Eds.; Wiley: Chichester, 1998; pp 1142−1157.

(42) Eckert, F.; Werner, H. J. *Theor. Chem. Acc.* **1998**, *100* (1−4), 21−30.

(43) Dennis, J. E.; Schnabel, R. B. *Numerical Methods for Unconstrained Optimization and Nonlinear Equations*; Prentice Hall: Englewood Cliffs, NJ, 1983.

(44) Fletcher, R. *Practical Methods of Optimization*; Wiley: Chichester, 1987.

(45) Anglada, J. M.; Bofill, J. M. *J. Comput. Chem.* **1998**, *19* (3), 349−362.

(46) Bofill, J. M. *J. Comput. Chem.* **1994**, *15* (1), 1−11.

(47) Farkas, Ö.; Schlegel, H. B. *J. Chem. Phys.* **1999**, *111* (24), 10806−10814.

(48) Farkas, Ö.; Schlegel, H. B. *Phys. Chem. Chem. Phys.* **2002**, *4* (1), 11−15.

(49) Frisch, M. J.; Trucks, G. W.; Schlegel, H. B.; Scuseria, G. E.; Robb, M. A.; Cheeseman, J. R.; Montgomery, J. A., Jr.,; Vreven, T.; Kudin, K. N.; Burant, J. C.; Millam, J. M.; Iyengar, S. S.; Tomasi, J.; Barone, V.; Mennucci, B.; Cossi, M.; Scalmani, G.; Rega, N.; Petersson, G. A.; Nakatsuji, H.; Hada, M.; Ehara, M.; Toyota, K.; Fukuda, R.; Hasegawa, J.; Ishida, M.; Nakajima, T.; Honda, Y.; Kitao, O.; Nakai, H.; Klene, M.; Li, X.; Knox, J. E.; Hratchian, H. P.; Cross, J. B.; Adamo, C.; Jaramillo, J.; Gomperts, R.; Stratmann, R. E.; Yazyev, O.; Austin, A. J.; Cammi, R.; Pomelli, C.; Ochterski, J. W.; Ayala, P. Y.; Morokuma, K.; Voth, G. A.; Salvador, P.; Dannenberg, J. J.; Zakrzewski, V. G.; Dapprich, S.; Daniels, A. D.; Strain, M. C.; Farkas, O.; Malick, D. K.; Rabuck, A. D.; Raghavachari, K.; Foresman, J. B.; Ortiz, J. V.; Cui, Q.; Baboul, A. G.; Clifford, S.; Cioslowski, J.; Stefanov, B. B.; Liu, G.; Liashenko, A.; Piskorz, P.; Komaromi, I.; Martin, R. L.; Fox, D. J.; Keith, T.; Al-Laham, M. A.; Peng, C. Y.; Nanayakkara, A.; Challacombe, M.; Gill, P. M. W.; Johnson, B.; Chen, W.; Wong, M. W.; Gonzalez, C.; Pople, J. A. Gaussian, Inc.: Pittsburgh, PA, 2003.

(50) Collins, J. B.; Schleyer, P. v. R.; Binkley, J. S.; Pople, J. A. *J. Chem. Phys.* **1976**, *64*, 5142.

(51) Hehre, W. J.; Stewart, R. F.; Pople, J. A. *J. Chem. Phys.* **1969**, *51*, 2657.

(52) Binkley, J. S.; Pople, J. A.; Hehre, W. J. *J. Am. Chem. Soc.* **1980**, *102*, 939.

(53) Gordon, M. S.; Binkley, J. S.; Pople, J. A.; Pietro, W. J.; Hehre, W. J. *J. Am. Chem. Soc.* **1982**, *104*, 2797.

(54) Pietro, W. J.; Francl, M. M.; Hehre, W. J.; Defrees, D. J.; Pople, J. A.; Binkley, J. S. *J. Am. Chem. Soc.* **1982**, *104*, 5039.

(55) Ditchfield, R.; Hehre, W. R.; Pople, J. A. *J. Chem. Phys.* **1971**, *54*, 724.

(56) Gordon, M. S. *Chem. Phys. Lett.* **1980**, *76*, 163.

(57) Hariharan, P. C.; Pople, J. A. *Theor. Chim. Acta* **1973**, *28*, 213.

(58) Hariharan, P. C.; Pople, J. A. *Mol. Phys.* **1974**, *27*, 209.

(59) Hehre, W. J.; Ditchfield, R.; Pople, J. A. *J. Chem. Phys.* **1972**, *56*, 2257.

(60) Niu, S. Q.; Hall, M. B. *Chem. Rev.* **2000**, *100* (2), 353−405.

(61) Niu, S. Q.; Hall, M. B. *J. Am. Chem. Soc.* **1997**, *119* (13), 3077−3086.

(62) Niu, S. Q.; Hall, M. B. *J. Phys. Chem. A* **1997**, *101* (7), 1360−1365.

(63) Lee, C. T.; Yang, W. T.; Parr, R. G. *Phys. Rev. B* **1988**, *37* (2), 785−789.

(64) Becke, A. D. *J. Chem. Phys.* **1993**, *98*, 5648.

(65) Krishnan, R.; Binkley, J. S.; Seeger, R.; Pople, J. A. *J. Chem. Phys.* **1980**, *72*, 650.

(66) McLean, A. D.; Chandler, G. S. *J. Chem. Phys.* **1980**, *72*, 5639.

CT0499783